



THE MORE YOU  
**IMAGE**  
THE MORE YOU  
UNDERSTAND



Quantum GX2 microCT

### Automate bone mineral density calculations.

Without question, microCT is the go-to modality for bone imaging, and bone-research applications such as osteoarthritis and osteoporosis use bone mineral density (BMD) as a readout for the disease state. Discover how the Quantum GX2 microCT imaging system and AccuCT™ advanced bone-analysis software can be used to automatically calibrate BMD scans, saving you time, while improving consistency across analyses.



Download Technical Note



**PerkinElmer**  
For the Better

# Greater Gains in Spine and Hip Strength for Romosozumab Compared With Teriparatide in Postmenopausal Women With Low Bone Mass

Tony M Keaveny,<sup>1</sup> Daria B Crittenden,<sup>2</sup> Michael A Bolognese,<sup>3</sup> Harry K Genant,<sup>4</sup> Klaus Engelke,<sup>5</sup> Beatriz Oliveri,<sup>6</sup> Jacques P Brown,<sup>7</sup> Bente L Langdahl,<sup>8</sup> Chris Yan,<sup>9</sup> Andreas Grauer,<sup>2</sup> and Cesar Libanati<sup>10</sup>

<sup>1</sup>University of California, Berkeley, CA, USA

<sup>2</sup>Amgen Inc., Thousand Oaks, CA, USA

<sup>3</sup>The Bethesda Health Research Center, Bethesda, MD, USA

<sup>4</sup>UCSF and Synarc Inc., San Francisco, CA, USA

<sup>5</sup>Bioclinica, Hamburg, Germany, and Institute of Medical Physics, University of Erlangen, Erlangen, Germany

<sup>6</sup>Hospital de Clínicas, INIGEM, Buenos Aires, Argentina

<sup>7</sup>CHU de Québec Research Centre and Laval University, Québec City, QC, Canada

<sup>8</sup>Aarhus University Hospital, Aarhus, Denmark

<sup>9</sup>Amgen Ltd., Cambridge, UK

<sup>10</sup>UCB BioPharma, Brussels, Belgium

## ABSTRACT

Romosozumab is a monoclonal antibody that inhibits sclerostin and has been shown to reduce the risk of fractures within 12 months. In a phase II, randomized, placebo-controlled clinical trial of treatment-naïve postmenopausal women with low bone mass, romosozumab increased bone mineral density (BMD) at the hip and spine by the dual effect of increasing bone formation and decreasing bone resorption. In a substudy of that trial, which included placebo and teriparatide arms, here we investigated whether those observed increases in BMD also resulted in improvements in estimated strength, as assessed by finite element analysis. Participants received blinded romosozumab s.c. (210 mg monthly) or placebo, or open-label teriparatide (20 µg daily) for 12 months. CT scans, obtained at the lumbar spine ( $n = 82$ ) and proximal femur ( $n = 46$ ) at baseline and month 12, were analyzed with finite element software (VirtuOst, O.N. Diagnostics) to estimate strength for a simulated compression overload for the spine (L<sub>1</sub> vertebral body) and a sideways fall for the proximal femur, all blinded to treatment assignment. We found that, at month 12, vertebral strength increased more for romosozumab compared with both teriparatide (27.3% versus 18.5%;  $p = 0.005$ ) and placebo (27.3% versus -3.9%;  $p < 0.0001$ ); changes in femoral strength for romosozumab showed similar but smaller changes, increasing more with romosozumab versus teriparatide (3.6% versus -0.7%;  $p = 0.027$ ), and trending higher versus placebo (3.6% versus -0.1%;  $p = 0.059$ ). Compartmental analysis revealed that the bone-strengthening effects for romosozumab were associated with positive contributions from both the cortical and trabecular bone compartments at both the lumbar spine and hip. Taken together, these findings suggest that romosozumab may offer patients with osteoporosis a new bone-forming therapeutic option that increases both vertebral and femoral strength within 12 months. © 2017 American Society for Bone and Mineral Research.

**KEY WORDS:** OSTEOPOROSIS; ANABOLICS; ROMOSUZUMAB; TERIPARATIDE

## Introduction

Osteoporosis is characterized by loss of bone mass and impairment of bone architecture, which decreases bone strength and increases risk of fracture.<sup>(1)</sup> Improving bone mass and strength is imperative in managing patients at risk for fracture.

While antiresorptive therapies remain the most commonly used agents to treat osteoporosis, new anabolic or bone-forming agents under development are likely to be soon available in the clinic. Antiresorptive therapies reduce bone remodeling by

inhibiting osteoclast function, whereas bone-forming therapy improves bone mass by stimulating or promoting bone formation. Teriparatide is a US-approved bone-forming agent and works by increasing both remodeling and modeling activity on bone surfaces.<sup>(2)</sup> Although teriparatide increases trabecular bone mineral density (BMD) at the hip and spine,<sup>(3-6)</sup> the increase in bone resorption during up to 24 months of treatment has been associated with a decrease in volumetric BMD (vBMD) of the cortical bone at the hip<sup>(3,4)</sup>—presumably because of an increase in cortical porosity.<sup>(7,8)</sup> Thus, there is clinical interest in the

Received in original form January 24, 2017; revised form May 9, 2017; accepted May 22, 2017. Accepted manuscript online May 25, 2017.

Address correspondence to: Tony M Keaveny, PhD, Departments of Mechanical Engineering and Bioengineering, 5124 Etchervy Hall, MC 1740, University of California, Berkeley, CA 94720-1740, USA. E-mail: tonykeaveny@berkeley.edu

Journal of Bone and Mineral Research, Vol. 32, No. 9, September 2017, pp 1956–1962

DOI: 10.1002/jbmr.3176

© 2017 American Society for Bone and Mineral Research

development of bone-forming agents that are associated with increases in mass of both the trabecular and cortical compartments and without any increase in cortical porosity.

Romosozumab is a monoclonal antibody that inhibits sclerostin with a dual effect on bone, increasing bone formation on modeling and remodeling surfaces while decreasing bone resorption, and has been shown to reduce the risk of fractures within 1 year of treatment.<sup>(9)</sup> In a phase II clinical trial of postmenopausal women with low bone mass (NCT00896532), romosozumab was well tolerated and the dual effect was associated with larger gains in BMD, measured by dual-energy X-ray absorptiometry (DXA) imaging, compared with placebo and teriparatide.<sup>(10)</sup> In a quantitative computed tomography (QCT) analysis of a subset of these participants, the effect of romosozumab was assessed on vBMD and bone mineral content (BMC) at the lumbar spine and total hip, and romosozumab was found to significantly increase integral vBMD and BMC at both sites from baseline and compared with both placebo and teriparatide groups.<sup>(11)</sup> These findings were consistent with preclinical studies that showed increased bone mass after sclerostin inhibition, which also was associated with increased bone strength.<sup>(12,13)</sup> Because finite element analysis (FEA) can provide a noninvasive assessment of strength changes after treatment,<sup>(14)</sup> we sought to evaluate how the changes in vBMD and BMC observed in this study influenced FEA-estimated strength at the spine and hip.

Here, we analyze this subset of participants from the phase II trial and report on changes in bone strength at the spine and hip assessed by FEA. FEA is a technique endorsed by official guidelines of the International Society for Clinical Densitometry (ISCD)<sup>(15)</sup> and accepted by the US FDA<sup>(14–17)</sup> to estimate whole-bone strength for assessment of fracture risk and monitoring of osteoporosis treatment.

## Materials and Methods

### Phase II study design and participants

The methods and primary results of this phase II randomized, placebo-controlled, parallel-group study have previously been

reported.<sup>(10,11)</sup> Briefly, 419 postmenopausal women aged 55 to 85 years with low BMD (ie, lumbar spine, total hip, or femoral neck *T*-scores between  $-2.0$  and  $-3.5$ ) were enrolled at 28 study centers. Patients were randomized to five dosing regimens each administered for 12 months: blinded romosozumab in subcutaneous dosages of 70 mg ( $n = 51$ ), 140 mg ( $n = 51$ ), or 210 mg ( $n = 52$ ) monthly, or 140 mg ( $n = 54$ ) or 210 mg ( $n = 53$ ) every 3 months; placebo administered subcutaneously either monthly ( $n = 30$ ) or every 3 months ( $n = 22$ ); open-label oral alendronate 70 mg weekly ( $n = 51$ ); or 20  $\mu\text{g}$  daily of subcutaneous teriparatide ( $n = 55$ ). All participants received daily calcium (1000 mg) and vitamin D (800 IU).

The study protocol was approved by an independent ethics committee or institutional review board at each study site before the study started. All subjects provided written, informed consent to participate in the trial.

### QCT substudy design

A subset of participants from the phase II study had QCT scans, and the results of this QCT substudy have been previously reported.<sup>(11)</sup> At study sites with suitable CT scanners, participants in each of the treatment groups were invited to participate in the QCT substudy before randomization, until the number of planned subjects was reached. Participants in the substudy had QCT scans of the lumbar spine (romosozumab 210 mg monthly  $n = 24$ ; placebo  $n = 27$ ; teriparatide daily  $n = 31$ ) (Fig. 1). These participants also underwent either a QCT scan of the hip (romosozumab  $n = 9$ ; placebo  $n = 18$ ; teriparatide  $n = 19$ ) or a specialized high-resolution QCT scan of the 12th thoracic vertebra (these high-resolution spine scans were not included in the current analysis). Given this study design, fewer participants had hip scans than lumbar spine scans, and the blinded randomization at the start of the study resulted in a different number of hip scans in each of the treatment groups.

### QCT assessment

Details on the QCT methodology are described elsewhere.<sup>(11)</sup> In brief, whole-body spiral CT scans ( $\geq 4$  detector rows) were

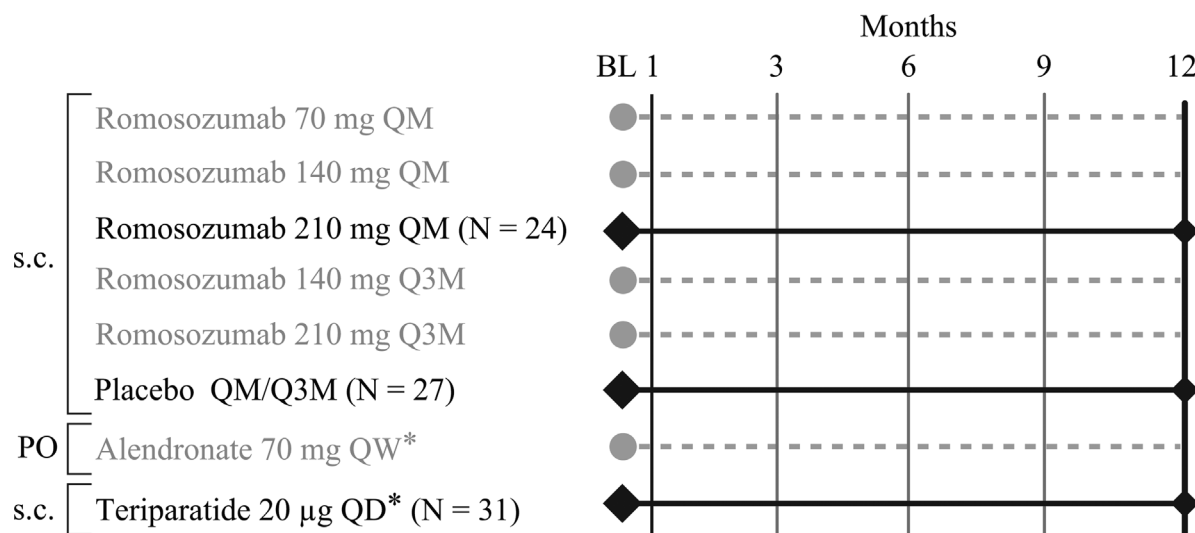


**Fig. 1.** Study schema. N = subjects with QCT scan at lumbar spine or hip at baseline and post baseline. \*Open-label administration. BL = baseline; PO = orally; QD = daily; QM = monthly; Q3M = once every 3 months; QW = weekly.

performed at the lumbar spine (L<sub>1</sub> to L<sub>2</sub>) and total hip at baseline and month 12, the patient lying on a Mindways calibration phantom (Mindways Software Inc., Austin, TX, USA) during scanning. Scans were performed at 120 kV with a pitch of 1 (or close to 1), using defaults of 100 and 170 mAs for the spine and hip, respectively, and were reconstructed at 1.0-mm (or 1.25-mm) slice thickness, using a 36- or 40-cm field of view for the spine and hip, respectively, and a medium kernel. Scanner cross-calibration and stability were assessed using the Mindways QA phantom and the European Spine Phantom (ESP, QRM GmbH, Möhrendorf, Germany).

### FEA assessment

We applied FEA to all participants who had a baseline and postbaseline QCT scan of either the spine or hip. For each participant, we estimated the changes in strength compared with baseline for the whole bone, and the trabecular and cortical compartments, blinded-to-treatment, using the VirtuOst software (O.N. Diagnostics, Berkeley, CA, USA) as previously described.<sup>(16)</sup> Briefly, after segmenting, calibrating, registering, and resampling the images, the scans were converted into finite element models by converting image voxels into cube-shaped finite elements (1.0 mm size for the spine, 1.5 mm for the hip; both approaches producing finite element models having approximately 40,000 elements). For the lumbar spine, a thin layer of plastic was virtually applied over each endplate through which the vertebral body was loaded to simulate failure for a uniform compressive overload. For the hip, an unprotected sideways fall was simulated, the diaphysis angled at 15° to the ground and 15° of internal rotation. For both sites, the bones were virtually loaded to failure to estimate the breaking strength (defined from the resulting nonlinear force-deformation curves as the force at 1.9% and 4.0% overall deformation for the spine and hip, respectively).

To provide mechanistic insight into the biomechanical mode of action of the treatments, additional controlled variations of

these models were performed to provide estimates of the changes in overall strength associated with changes in only the cortical and trabecular compartments. Lumbar spine trabecular strength was computed using models that had the outer 2 mm of bone virtually removed. Lumbar spine cortical strength was calculated as the overall spine strength minus the spine trabecular strength. Hip cortical strength was computed using models that had all the bone in the trabecular compartment converted into (a low-stiffness) plastic, leaving the bone within the cortical compartment unaltered. Hip trabecular strength was computed using models that had all the bone in the cortical compartment at each time point converted into plastic (a stiffer plastic for the bone having an apparent density of more than 1.0 g/cm<sup>3</sup> and a less stiff plastic for the remaining bone), leaving the bone within the trabecular compartment unaltered (Fig. 2). For the hip, the trabecular compartment was defined as all the bone within 3 mm of the outer surface, minus any bone having an apparent density of more than 1.0 g/cm<sup>3</sup>; the cortical compartment was all other bone.

### Statistical analyses

All patients with a baseline and postbaseline QCT FEA measurement by month 12 were included in this analysis. There was no imputation of missing data. Following a prespecified statistical plan, the percentage changes from baseline in strength to month 12 at the lumbar spine and hip were estimated using an analysis of covariance (ANCOVA) model, with baseline QCT FEA value, treatment (categorical), and geographic region as the independent variables. Least square means and associated 95% confidence intervals (CIs) for each treatment were determined. Because the overall analysis was considered exploratory, pairwise comparisons of the adjusted means between the treatment groups were tested at month 12 without adjusting for multiplicity. All statistical analyses were conducted using SAS software v9.3 (SAS Institute, Cary, NC, USA).

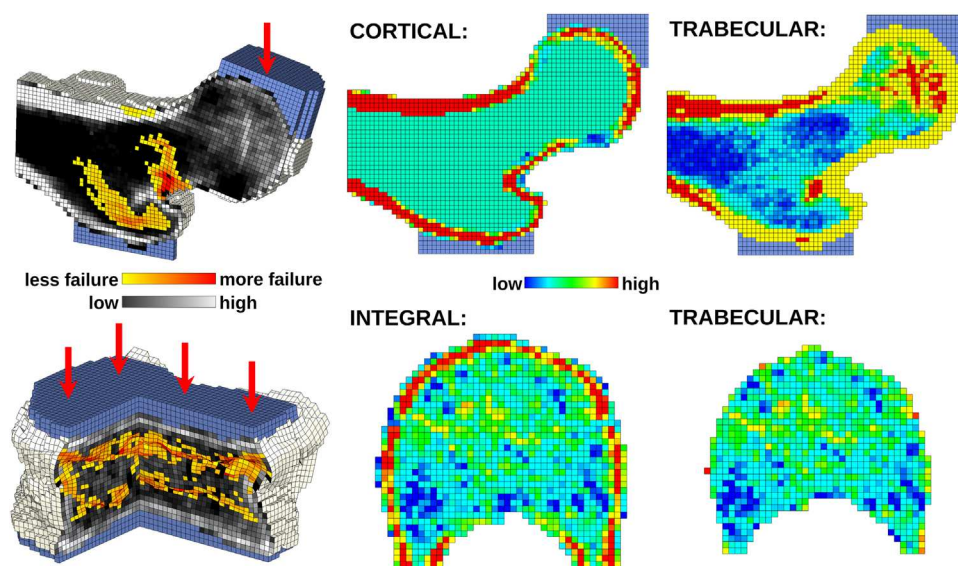


**Fig. 2.** Example of finite element models for a 68-year-old subject at baseline. 3D cut-out views depict the distribution of volumetric BMD (grayscale) and regions of failure (colored) under virtual loading via a thin layer of plastic (blue) for a sideways fall for the hip (top) and for a compressive overload for the spine (bottom); virtual deformations are magnified for viewing purposes. 2D sections from the full models that were used for estimating strength changes due only to treatment effects on the individual trabecular and cortical compartments (color shows material properties).

## Results

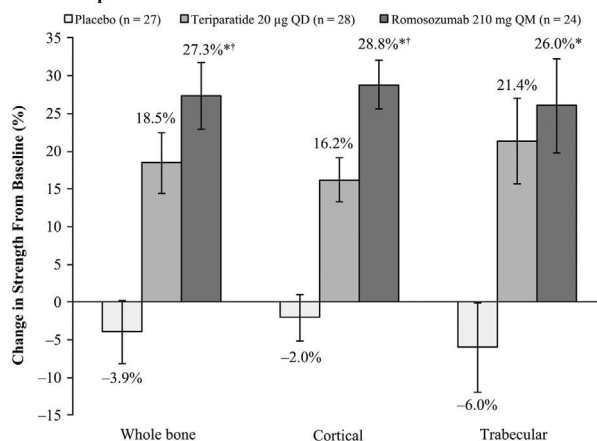
The baseline characteristics of this subset were generally similar across treatment groups (Table 1) and similar to the overall study population.<sup>(10)</sup> The mean age of participants was 65.5 years, with mean *T*-scores at baseline of  $-2.4$  at the lumbar spine and  $-1.3$  at the hip.

At 12 months, romosozumab significantly increased vertebral and femoral strength compared with baseline for the whole bone and the cortical and trabecular compartments (all  $p < 0.03$ ; Fig. 3). From baseline, vertebral strength increased by 27.3% with romosozumab (Fig. 3A), and this change was greater than the 18.5% increase with teriparatide (difference between romosozumab and teriparatide of 8.9%;  $p = 0.005$ ) and the 3.9% decrease with placebo (difference between romosozumab and placebo of 31.2%;  $p < 0.0001$ ). Despite the small sample size of the romosozumab group, romosozumab also significantly increased femoral strength by 3.6% compared with baseline ( $p = 0.026$ ; Fig. 3B), which was greater than the  $-0.7\%$  nonsignificant change from baseline with teriparatide (difference from romosozumab 4.3%;  $p = 0.027$ ) and the nonsignificant change of  $-0.1\%$  with placebo (difference from romosozumab 3.7%;  $p = 0.059$ ).

Further analysis of the FEA models showed that the strengthening effect observed with romosozumab at 12 months was due to positive contributions from both the cortical and trabecular bone compartments. At the lumbar spine, strength associated with the cortical compartment increased from baseline by 28.8% with romosozumab ( $p < 0.0001$ ) and 16.2% with teriparatide ( $p < 0.0001$ ) and decreased by 2.0% with placebo ( $p = 0.188$ ), which corresponded to significantly greater increases in cortical strength with romosozumab compared with both the teriparatide ( $p < 0.0001$ ) and placebo ( $p < 0.0001$ ) groups. Also, at the spine, strength in the trabecular compartment increased by 26.0% with romosozumab ( $p < 0.0001$ ) and 21.4% with teriparatide ( $p < 0.0001$ ) and decreased by 6.0% with placebo ( $p = 0.047$ ), resulting in a significantly greater increase in trabecular strength with romosozumab compared with placebo ( $p < 0.0001$ ).

At the hip, strength in the cortical compartment significantly increased from baseline to month 12 by 2.4% with romosozumab ( $p = 0.01$ ) and changed nonsignificantly by 0.2% with both teriparatide and placebo; these changes were greater for

### A. Lumbar spine



### B. Hip

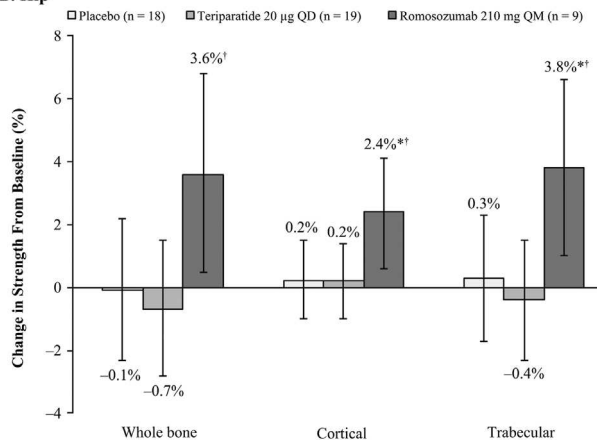


**Fig. 3.** Mean percentage changes (95% CI) in FEA strength at month 12 for (A) lumbar spine and (B) hip. An ANCOVA model was used to compare the treatment arms from baseline to month 12. \* $p < 0.05$  compared with placebo; † $p < 0.05$  compared with teriparatide. QD = daily; QM = monthly. Significance from baseline not shown. *n* = number of subjects randomized to QCT substudy and had baseline and at least one post-baseline QCT FEA measurements on or before month 12.

**Table 1.** Baseline Characteristics

	Placebo ( <i>n</i> = 27)	Teriparatide 20 µg QD ( <i>n</i> = 31)	Romosozumab 210 mg QM ( <i>n</i> = 24)
Mean age (SD), years	66.1 (5.8)	65.8 (5.7)	64.3 (4.7)
Mean lumbar spine values (SD)			
DXA aBMD <i>T</i> -score	-2.3 (0.6)	-2.3 (0.5)	-2.5 (0.5)
QCT vBMD, mg/cm <sup>3</sup>	170 (19)	172 (21)	164 (19)
FEA strength, Newtons	4344 (932)	4523 (717)	4165 (610)
Mean total hip values (SD)			
DXA BMD <i>T</i> -score	-1.3 (0.6)	-1.2 (0.8)	-1.4 (0.6)
QCT vBMD, mg/cm <sup>3</sup>	251 (28)	249 (38)	243 (21)
FEA strength, Newtons	3285 (425)	3415 (508)	3331 (313)
Serum P1NP concentration, µg/L			
Median (IQR)	49.4 (37.9–62.7)	47.6 (42.5–58.6)	51.6 (41.0–62.5)
Serum CTx-1 concentration, ng/mL			
Median (IQR)	0.5 (0.4–0.7)	0.5 (0.4–0.6)	0.5 (0.4–0.6)

aBMD = areal BMD; FEA = finite element analysis; IQR = interquartile range; *n* = number of subjects randomized to the QCT substudy; QD = daily; QM = monthly; vBMD = volumetric BMD.

romosozumab than for both teriparatide ( $p = 0.045$ ) and placebo ( $p = 0.048$ ). For the trabecular compartment at the hip, strength increased significantly by 3.8% with romosozumab ( $p = 0.01$ ) and changed insignificantly by  $-0.4\%$  and  $0.3\%$ , respectively, with both teriparatide and placebo; these changes were greater for romosozumab than for both teriparatide ( $p = 0.016$ ) and placebo ( $p = 0.042$ ).

## Discussion

In this study of postmenopausal women with low bone mass, 12 months of treatment with romosozumab significantly increased both vertebral and femoral strength from baseline and also compared with treatment with teriparatide. These larger gains in strength with romosozumab treatment were consistent with the gains that occurred in areal BMD (aBMD), as measured by DXA in the same subjects from this QCT substudy cohort,<sup>(11)</sup> which in turn were consistent with the aBMD gains observed in the parent phase II trial.<sup>(10)</sup> Positive gains in strength at the spine and hip after 12 months of treatment with romosozumab extend to humans the preclinical data showing that inhibition of sclerostin was associated with significant and rapid improvements—after 6 or 26 weeks—in bone strength at the spine, femoral diaphysis, and femoral neck in rats.<sup>(12)</sup>

The FEA analysis provides insight into how changes in overall BMD and bone mass at the spine and hip are expected to relate to changes in whole-bone strength. In the QCT substudy for this cohort,<sup>(11)</sup> changes in total hip aBMD were 3.9%, 0.8%, and  $-0.7\%$  for romosozumab, teriparatide, and placebo, respectively. These changes closely corresponded with the changes in BMC as measured by DXA (3.9%, 1.3%,  $-0.4\%$ ), with the changes in both integral vBMD (4.1%, 1.2%, 0.3%) and BMC (4.7%, 0.8%, 1.1%) as measured by QCT, and also were consistent with the mean changes in femoral estimated strength (3.6%,  $-0.7\%$ ,  $-0.1\%$ , respectively). Thus, at the hip, the average changes in mass and density as measured by DXA and QCT corresponded to the changes in overall bone strength, an observation that is relevant to interpreting how treatment-induced changes in BMD might be associated with changes in risk of fracture at the hip. By contrast, the changes measured for the total spine (mean of L<sub>1</sub> to L<sub>4</sub> vertebrae, posterior elements included) by DXA both for aBMD (12.3%, 6.9%,  $-0.4\%$  for romosozumab, teriparatide, and placebo, respectively) and BMC (14.9%, 8.6%,  $-0.2\%$ , respectively) underestimated the changes for the vertebral body (mean of L<sub>1</sub> and L<sub>2</sub> vertebrae, no posterior elements) as measured by QCT both for integral vBMD (17.7%, 12.9%,  $-0.8\%$ ) and BMC (17.7%, 12.8%,  $-1.0\%$ ).<sup>(11)</sup> Furthermore, unlike at the hip, these changes in BMD and BMC at the spine underestimated the changes in strength (L<sub>1</sub> vertebra, no posterior elements) as estimated by FEA (27.3%, 18.5%,  $-3.9\%$ ). In general, the relation between changes in mean BMD (or bone mass) and changes in whole-bone strength depends on the spatial distribution of the changes in BMD including relative changes in the cortical versus trabecular compartments, any changes in geometry, the relation between BMD and bone material properties (which is nonlinear), the external loading conditions of the bone, as well as the internal load transfer patterns within the bone, which results from bone macro- and microarchitecture. These collective findings demonstrate this complexity and suggest that greater increases in whole-bone strength can be expected with these treatments at the spine (for a compressive load) than at the

hip (for a sideways fall) for any observed changes in average BMD or bone mass.

Biomechanically, the FEA analysis also provides unique mechanistic insight into how changes in the individual trabecular and cortical compartments might independently contribute to changes in overall whole-bone strength. For example, at the spine, the changes in vertebral strength attributed to changes in the cortical compartment only (28.8% versus 16.2% for romosozumab and teriparatide, respectively) were more consistent with the reported changes from the QCT substudy in cortical bone mass (23.3% versus 10.9%) than in cortical vBMD (13.7% versus 5.7%).<sup>(11)</sup> The QCT study also reported that a large portion of the change in cortical mass for both romosozumab and teriparatide was due to an appreciable increase in cortical thickness for each treatment (22.7% versus 12.3%). Additional analyses (not reported) indicated no significant treatment-related changes in external geometry for the spine (or hip), implying that the treatment-induced increases in cortical thickness reported in the QCT substudy were due to the result of bone accretion at the endosteal surface of the cortex. Because of the way we defined the vertebral “cortical” compartment in our study—all bone within 2 mm of the periosteal surface—and because the true vertebral cortex is so thin, these endosteal cortical changes were captured within our “cortical” compartment, as were any changes in any adjacent trabecular bone within that 2-mm region. Supporting this approach to estimating the strength effects of changes in just the trabecular compartment at the spine, detailed micro-CT-based FEA has shown that when the thin vertebral cortex is removed, about 1 mm or more of adjacent trabecular bone loses its load-carrying ability because that bone is no longer attached to any load-bearing tissue.<sup>(18,19)</sup> In the current study, slightly larger strength increases occurred in the “cortical” than trabecular compartment for romosozumab, whereas for teriparatide slightly larger strength increases occurred in the trabecular compartment, an observation also noted with denosumab.<sup>(16)</sup> Thus, the biomechanical effect of romosozumab on the “cortical” compartment—and presumably the thin vertebral cortex—may be a differentiating attribute. Interestingly, in our study, there was a statistically significant decrease in the strength of the trabecular compartment for the placebo group that was not apparent from the QCT results,<sup>(11)</sup> perhaps indicative of a biomechanically relevant change in the spatial distribution of vBMD within the trabecular compartment.

Biologically, the increases in strength for romosozumab compared with teriparatide are likely the result of the different mechanisms of actions of these two treatments. Teriparatide stimulates remodeling and consequently also increases bone resorption. The increase in resorption with teriparatide can increase endosteal bone resorption and cortical porosity, at least temporarily, and thus counteract the gains associated with the bone accretion known to also occur.<sup>(8,20)</sup> Romosozumab has a dual effect, increasing bone formation and simultaneously decreasing bone resorption, via sclerostin inhibition.<sup>(10,21)</sup> Sclerostin is a negative regulator of bone formation by blocking Wnt signaling in bone and also increases bone resorption by promoting osteoclast formation and activity through augmented RANKL/OPG ratio.<sup>(22–24)</sup> QCT scans and FEA results from subjects treated with romosozumab indicate that these biological mechanisms result in improvements in both trabecular and cortical bone mass and in overall spine and hip strength; there may also be subtle changes in the spatial distribution of vBMD. Of note, significant gains in cortical strength at the hip

were observed within 1 year of romosozumab treatment, whereas no change in cortical strength was observed with teriparatide over the same time period, which is consistent with previous studies of teriparatide that reported either no change or a slight decrease in the strength associated with the hip cortical compartment.<sup>(4,5)</sup>

The main limitation of this study is the small sample size, particularly for the romosozumab group that received a QCT scan of the hip. Thus, although our observed hip strength increases were consistent with the hip BMD changes previously reported for the larger DXA cohort,<sup>(11)</sup> our FEA results should be interpreted with caution and merit confirmation in a larger trial. A second limitation is that FEA only provides estimates of bone strength and not direct destructive measurements. However, FEA estimates of strength have been validated clinically for fracture risk assessment in numerous fracture-outcome studies at both the hip and spine and in women and men.<sup>(17,25–32)</sup> FEA is now cleared by the FDA and endorsed by the ISCD<sup>(15)</sup> to assess spine and hip fracture risk and to monitor treatment changes, and a recent study of cynomolgus monkeys demonstrated that treatment effects with denosumab on vertebral strength as estimated by FEA were highly correlated with strength as measured by destructive mechanical testing ( $R^2=0.97$ ).<sup>(14)</sup> Furthermore, the results from the recent Fracture Study in Postmenopausal Women with Osteoporosis (FRAME)<sup>(9)</sup> on postmenopausal women with BMD-defined osteoporosis showed a 73% lower risk of incident vertebral fracture for those treated with romosozumab compared with placebo at 12 months, which is consistent with the large increases in vertebral strength shown here. A final limitation of the study is the use of teriparatide for only 1 year, which prevents comparisons with longer administration.

In summary, the results of this study indicate that romosozumab increased FEA-estimated bone strength at both the lumbar spine and hip over 12 months in comparison with placebo and teriparatide in postmenopausal women with low bone mass. These strength improvements suggest that the distinctive dual effect of romosozumab to increase bone formation and decrease bone resorption may offer patients with osteoporosis a new bone-forming therapeutic option to increase both vertebral and femoral strength within 12 months.

## Disclosures

TMK consulted for Amgen, O.N. Diagnostics, and AgNovos Healthcare, owns stock in O.N. Diagnostics, and has patents with O.N. Diagnostics. O.N. Diagnostics was paid by Amgen to perform the FEA analyses.

DBC, CY, and AG are employees of and have stock/stock options in Amgen.

MAB has consulted for Amgen and received payment for speaker services from Amgen.

HKG has received consulting fees or honorarium from Amgen, Lilly, Merck, Janssen, Pfizer, Regeneron, Clementia, MedImmune, BioMarin, AgNovos, Medtronic, and BioClinica.

KE has consulted for Amgen and Radius and is an employee of BioClinica.

BO has received honorarium from Amgen as a study investigator, consulted for Pfizer and Shire, and received payment for speaker services from Shire, TRB Pharma, Danone, GlaxoSmithKline, and Quimica Montpellier.

JPB has received grants from Amgen and Eli Lilly, has consulted for Amgen, Eli Lilly, and Merck, is a member of

advisory boards for Amgen, Eli Lilly, and Merck, received travel support from Amgen, and received payment for speaker services and the development of educational presentations from Amgen and Eli Lilly.

BLL has consulted for Amgen, UCB Pharma, Eli Lilly, and Merck, was an investigator on this study and payment was received by BLL's institution in relation to this study, received grants from Amgen, Novo Nordisk, and Orkla Health, and received payment for speaker services from Amgen, Eli Lilly, and Merck.

CL is an employee of and has stock/stock options in UCB Pharma.

## Acknowledgments

This study was funded by Amgen Inc., Astellas, and UCB Pharma. Medical writing assistance in the preparation of this manuscript was provided by Scott Forbes, PhD, on behalf of Oxford PharmaGenesis, with funding provided by Amgen Inc., and by Mandy Suggitt of Amgen Inc.

Authors' roles: Study design: AG and CL. Study conduct: AG. Data collection: MAB, BO, JPB, and BLL. Data analysis: TMK, KE, and CY. Data interpretation: TMK, DBC, CL, and KE. Drafting of the manuscript: TMK, DBC, and CL. Revising the manuscript content: all authors. Approving the final version of the manuscript: all authors. Study supervision and responsibility for the integrity of the data analysis: CY.

## References

1. Cosman F, de Beur SJ, LeBoff MS, et al. Clinician's guide to prevention and treatment of osteoporosis. *Osteoporos Int*. 2014;25(10):2359–81.
2. Papapoulos S, Makras P. Selection of antiresorptive or anabolic treatments for postmenopausal osteoporosis. *Nat Clin Pract Endocrinol Metab*. 2008;4(9):514–23.
3. Borggrefe J, Graeff C, Nickelsen TN, Marin F, Glüer CC. Quantitative computed tomographic assessment of the effects of 24 months of teriparatide treatment on 3D femoral neck bone distribution, geometry, and bone strength: results from the EUROFORS study. *J Bone Miner Res*. 2010;25(3):472–81.
4. Keaveny TM, Hoffmann PF, Singh M, et al. Femoral bone strength and its relation to cortical and trabecular changes after treatment with PTH, alendronate, and their combination as assessed by finite element analysis of quantitative CT scans. *J Bone Miner Res*. 2008;23(12):1974–82.
5. Keaveny TM, McClung MR, Wan X, Kopperdahl DL, Mitlak BH, Krohn K. Femoral strength in osteoporotic women treated with teriparatide or alendronate. *Bone*. 2012;50(1):165–70.
6. Kleerekoper M, Greenspan SL, Lewiecki EM, et al. Assessing the effects of teriparatide treatment on bone mineral density, bone microarchitecture, and bone strength. *J Bone Joint Surg Am*. 2014;96(11):e90.
7. Eriksen EF, Keaveny TM, Gallagher ER, Krege JH. Literature review: the effects of teriparatide therapy at the hip in patients with osteoporosis. *Bone*. 2014;67:246–56.
8. Ma YL, Zeng QQ, Chiang AY, et al. Effects of teriparatide on cortical histomorphometric variables in postmenopausal women with or without prior alendronate treatment. *Bone*. 2014;59:139–47.
9. Cosman F, Crittenden DB, Adachi JD, et al. Romosozumab treatment in postmenopausal women with osteoporosis. *N Engl J Med*. 2016;375(16):1532–43.
10. McClung MR, Grauer A, Boonen S, et al. Romosozumab in postmenopausal women with low bone mineral density. *N Engl J Med*. 2014;370(5):412–20.
11. Genant HK, Engelke K, Bolognese MA, et al. Effects of romosozumab compared with teriparatide on bone density and mass at the spine

- and hip in postmenopausal women with low bone mass. *J Bone Miner Res.* 2017;32(1):181–7.
12. Li X, Niu QT, Warmington KS, et al. Progressive increases in bone mass and bone strength in an ovariectomized rat model of osteoporosis after 26 weeks of treatment with a sclerostin antibody. *Endocrinology.* 2014;155(12):4785–97.
  13. Ominsky MS, Boyd SK, Varela A, et al. Romosozumab improves bone mass and strength while maintaining bone quality in ovariectomized cynomolgus monkeys. *J Bone Miner Res.* 2017;32(4):788–801.
  14. Lee DC, Varela A, Kostenuik PJ, Ominsky MS, Keaveny TM. Finite element analysis of denosumab treatment effects on vertebral strength in ovariectomized cynomolgus monkeys. *J Bone Miner Res.* 2016;31(8):1586–95.
  15. Zysset P, Qin L, Lang T, et al. Clinical use of quantitative computed tomography-based finite element analysis of the hip and spine in the management of osteoporosis in adults: the 2015 ISCD Official Positions-Part II. *J Clin Densitom.* 2015;18(3):359–92.
  16. Keaveny TM, McClung MR, Genant HK, et al. Femoral and vertebral strength improvements in postmenopausal women with osteoporosis treated with denosumab. *J Bone Miner Res.* 2014;29(1):158–65.
  17. Kopperdahl DL, Aspelund T, Hoffmann PF, et al. Assessment of incident spine and hip fractures in women and men using finite element analysis of CT scans. *J Bone Miner Res.* 2014;29(3):570–80.
  18. Eswaran SK, Bayraktar HH, Adams MF, et al. The micro-mechanics of cortical shell removal in the human vertebral body. *Comput Methods Appl Mech Eng.* 2007;196:3025–32.
  19. Eswaran SK, Gupta A, Adams MF, Keaveny TM. Cortical and trabecular load sharing in the human vertebral body. *J Bone Miner Res.* 2006;21(2):307–14.
  20. Jiang Y, Zhao JJ, Mitlak BH, Wang O, Genant HK, Eriksen EF. Recombinant human parathyroid hormone (1–34) [teriparatide] improves both cortical and cancellous bone structure. *J Bone Miner Res.* 2003;18(11):1932–41.
  21. Padhi D, Jang G, Stouch B, Fang L, Posvar E. Single-dose, placebo-controlled, randomized study of AMG 785, a sclerostin monoclonal antibody. *J Bone Miner Res.* 2011;26(1):19–26.
  22. Li X, Zhang Y, Kang H, et al. Sclerostin binds to LRP5/6 and antagonizes canonical Wnt signaling. *J Biol Chem.* 2005;280(20):19883–7.
  23. Poole KE, van Bezooijen RL, Loveridge N, et al. Sclerostin is a delayed secreted product of osteocytes that inhibits bone formation. *FASEB J.* 2005;19(13):1842–4.
  24. Wijenayaka AR, Kogawa M, Lim HP, Bonewald LF, Findlay DM, Atkins GJ. Sclerostin stimulates osteocyte support of osteoclast activity by a RANKL-dependent pathway. *PLoS One.* 2011;6(10):e25900.
  25. Amin S, Kopperdahl DL, Melton LJ 3rd, et al. Association of hip strength estimates by finite-element analysis with fractures in women and men. *J Bone Miner Res.* 2011;26(7):1593–600.
  26. Anderson DE, Demissie S, Allaire BT, et al. The associations between QCT-based vertebral bone measurements and prevalent vertebral fractures depend on the spinal locations of both bone measurement and fracture. *Osteoporos Int.* 2014;25(2):559–66.
  27. Danielson ME, Beck TJ, Karlamangla AS, et al. A comparison of DXA and CT based methods for estimating the strength of the femoral neck in post-menopausal women. *Osteoporos Int.* 2013;24(4):1379–88.
  28. Imai K, Ohnishi I, Matsumoto T, Yamamoto S, Nakamura K. Assessment of vertebral fracture risk and therapeutic effects of alendronate in postmenopausal women using a quantitative computed tomography-based nonlinear finite element method. *Osteoporos Int.* 2009;20(5):801–10.
  29. Keyak JH, Sigurdsson S, Karlsdottir G, et al. Male-female differences in the association between incident hip fracture and proximal femoral strength: a finite element analysis study. *Bone.* 2011;48(6):1239–45.
  30. Melton LJ 3rd, Riggs BL, Keaveny TM, et al. Structural determinants of vertebral fracture risk. *J Bone Miner Res.* 2007;22(12):1885–92.
  31. Melton LJ 3rd, Riggs BL, Keaveny TM, et al. Relation of vertebral deformities to bone density, structure, and strength. *J Bone Miner Res.* 2010;25(9):1922–30.
  32. Orwoll ES, Marshall LM, Nielson CM, et al. Finite element analysis of the proximal femur and hip fracture risk in older men. *J Bone Miner Res.* 2009;24(3):475–83.